

January 25, 2016



Middle Fork Willamette River

Topobathymetric LiDAR Technical Data Report



Oregon LiDAR Consortium

Jake Edwards

Oregon Department of Geology and Mineral Industries

800 NE Oregon Street #28, Suite 965

Portland, OR 97232

PH: 971-673-1557



QSI Corvallis

517 SW 2nd St., Suite 400

Corvallis, OR 97333

PH: 541-752-1204

TABLE OF CONTENTS

INTRODUCTION	1
Deliverable Products	2
ACQUISITION	4
Sensor Selection: the Riegl VQ-820-G	4
Planning.....	4
Airborne LiDAR Survey	7
Ground Control.....	8
Monumentation	8
Ground Survey Points (GSPs).....	9
PROCESSING	11
Topobathymetric LiDAR Data	11
Bathymetric Refraction	13
LiDAR Derived Products.....	13
Topobathymetric DEMs	13
Intensity Images.....	13
RESULTS & DISCUSSION.....	15
Mapped Bathymetry and Depth Penetration.....	15
LiDAR Point Density.....	19
First Return Point Density.....	19
Bathymetric and Ground Classified Point Densities	22
LiDAR Accuracy Assessments	24
LiDAR Absolute Accuracy	24
LiDAR Relative Vertical Accuracy	27
CERTIFICATIONS	28
SELECTED IMAGES.....	29
GLOSSARY	32
APPENDIX A - ACCURACY CONTROLS	33

Cover Photo: View of the Willamette River at Pengra Road. The foreground is the gridded ground and bathymetry classified LiDAR returns colored by height. The background contains the addition of above ground LiDAR returns colored by intensity.

INTRODUCTION

This photo taken by QSI acquisition staff shows a view of the Middle Fork Willamette River in Oregon.



In September 2015, Quantum Spatial (QSI) was contracted by the Oregon LiDAR Consortium (OLC) to collect topobathymetric Light Detection and Ranging (LiDAR) data in the fall of 2015 for the Middle Fork Willamette River site in Oregon. The Middle Fork Willamette River area of interest stretches between Eugene/Springfield and Dexter Dam and Fall Creek below Fall Creek Dam. Traditional near-infrared (NIR) LiDAR was fully integrated with green wavelength return data (bathymetric) LiDAR in order to provide seamless and complete project mapping. Data were collected to aid OLC in providing a complete topobathymetric dataset to be used in analyses of the long term impacts associated with sediment deposition on downstream habitat and channel morphology.

This report accompanies the delivered topobathymetric LiDAR data, and documents contract specifications, data acquisition procedures, processing methods, and analysis of the final dataset including LiDAR accuracy, depth penetration, and density. Acquisition dates and acreage are shown in Table 1, the project extent is shown in Figure 1, and a complete list of contracted deliverables provided to OLC is shown in Table 2.

Table 1: Acquisition dates, acreage, and data types collected on the Middle Fork Willamette River site

Project Site	Contracted Acres	Buffered Acres	Acquisition Dates	Data Type
Middle Fork Willamette River	11,184	12,915	09/14/2015 – 09/15/2015	Topobathymetric LiDAR

Deliverable Products

Table 2: Products delivered to OLC for the Middle Fork Willamette River site

Middle Fork Willamette River Products	
Projection: UTM Zone 10 North	
Horizontal Datum: NAD83 (2011)	
Vertical Datum: NAVD88 (GEOID12A)	
Units: Meters	
Topobathymetric LiDAR	
Points	LAS v 1.2 <ul style="list-style-type: none"> Topobathymetric Integrated All Returns*
Rasters	1.0 Meter ESRI Grids <ul style="list-style-type: none"> Topobathymetric Model (unclipped & clipped) Highest Hit Model Depth Models 0.5 Meter GeoTiffs <ul style="list-style-type: none"> Green Wavelength Intensity Images ($\lambda = 532\text{nm}$) NIR Wavelength Intensity Images ($\lambda = 1,064\text{nm}$)
Vectors	Shapefiles (*.shp) <ul style="list-style-type: none"> LiDAR Boundary LiDAR Tile Indices* DEM Tile Index Water's Edge Polygon Bathymetric Confidence Polygon Ground Control Point Data

**Due to the large file size of the integrated dataset when delineated in 1/100th USGS quads, data is also being delivered in 500m tiles for ease of use.*

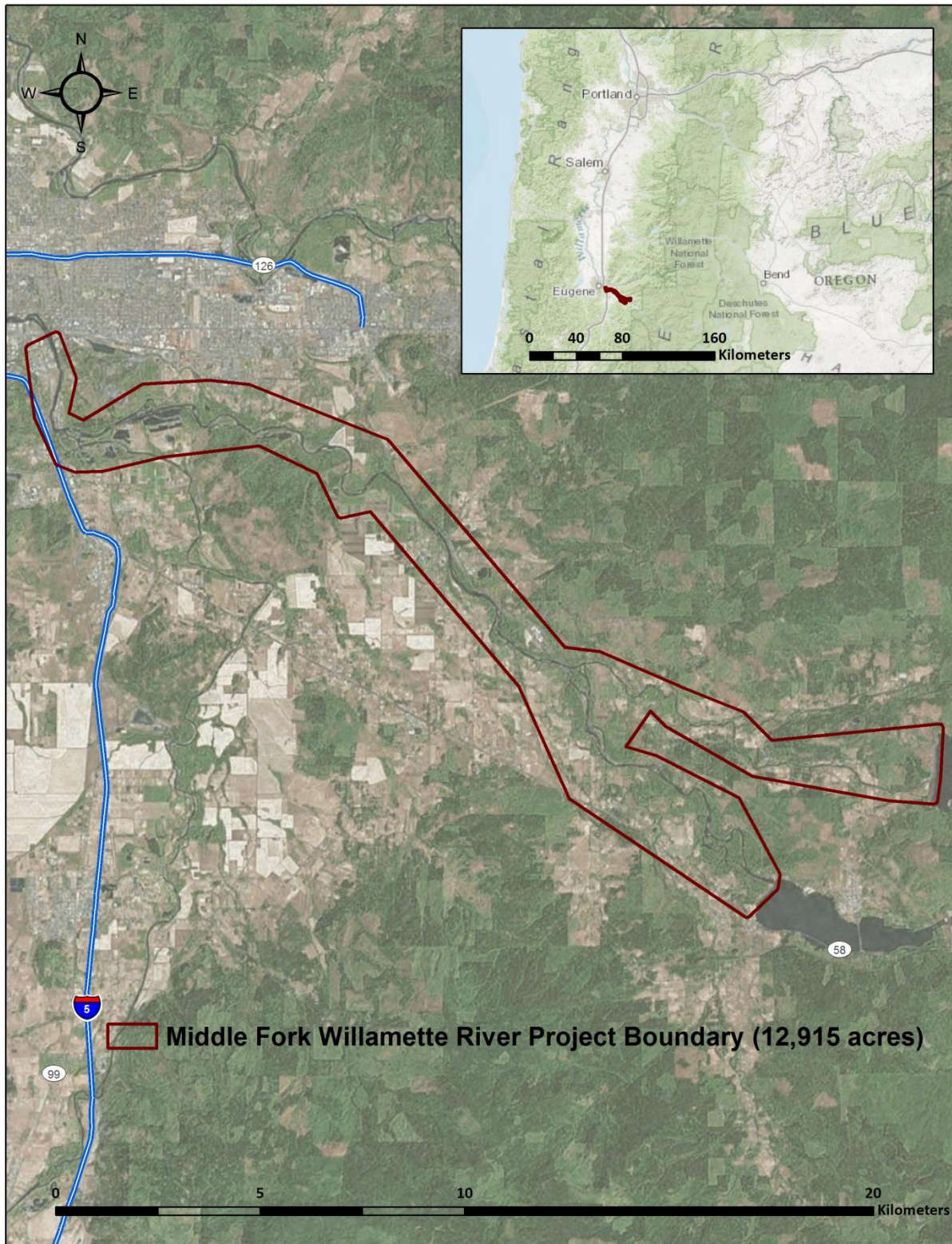


Figure 1: Location map of the Middle Fork Willamette River site in Oregon

QSI's Cessna Caravan



Sensor Selection: the Riegl VQ-820-G

The Riegl VQ-820-G was selected as the hydrographic airborne laser scanner for the Middle Fork Willamette River project based on fulfillment of several considerations deemed necessary for effective mapping of the project site. A high repetition pulse rate, high scanning speed, small laser footprint, and wide field of view allow for seamless collection of high resolution data of both topographic and bathymetric surfaces. A short laser pulse length allows for discrimination of underwater surface expression in shallow water, critical to shallow and dynamic environments such as the Willamette River. Sensor specifications and settings for the Middle Fork Willamette River acquisition are displayed in Table 6.

Planning

In preparation for data collection, QSI reviewed the project area and developed a specialized flight plan to ensure complete coverage of the Middle Fork Willamette River LiDAR study area at the target point density of ≥ 4.0 points/m² for green LiDAR returns, and ≥ 6.0 points/m² for NIR LiDAR returns (determined by the altitude required for flying topo-bathymetry). Acquisition parameters including orientation relative to terrain, flight altitude, pulse rate, scan angle, and ground speed were adapted to optimize flight paths and flight times while meeting all contract specifications.

Factors such as satellite constellation availability and weather windows must be considered during the planning stage. Any weather hazards or conditions affecting the flight were continuously monitored due to their potential impact on the daily success of airborne and ground operations. In addition, logistical considerations including private property access and potential air space restrictions, and channel flow rates (Figure 2 and Figure 3), and water clarity were reviewed.

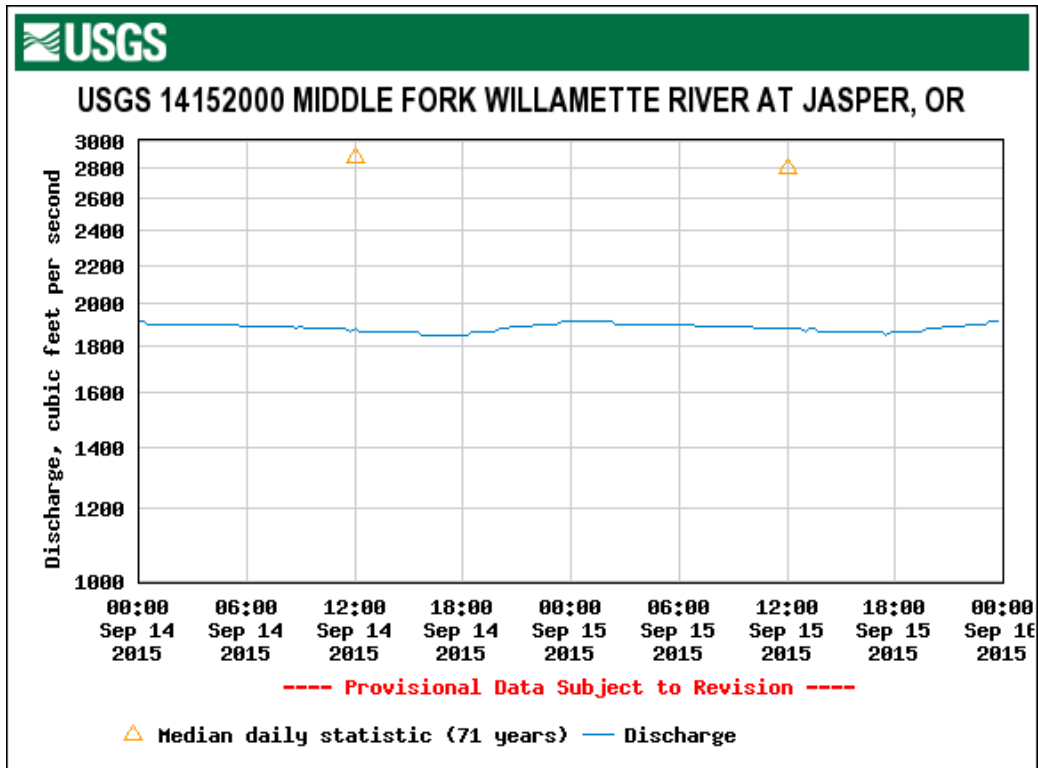


Figure 2: USGS Station 14152000 flow rate along the MF Willamette River near Jasper at the time of LiDAR acquisition.

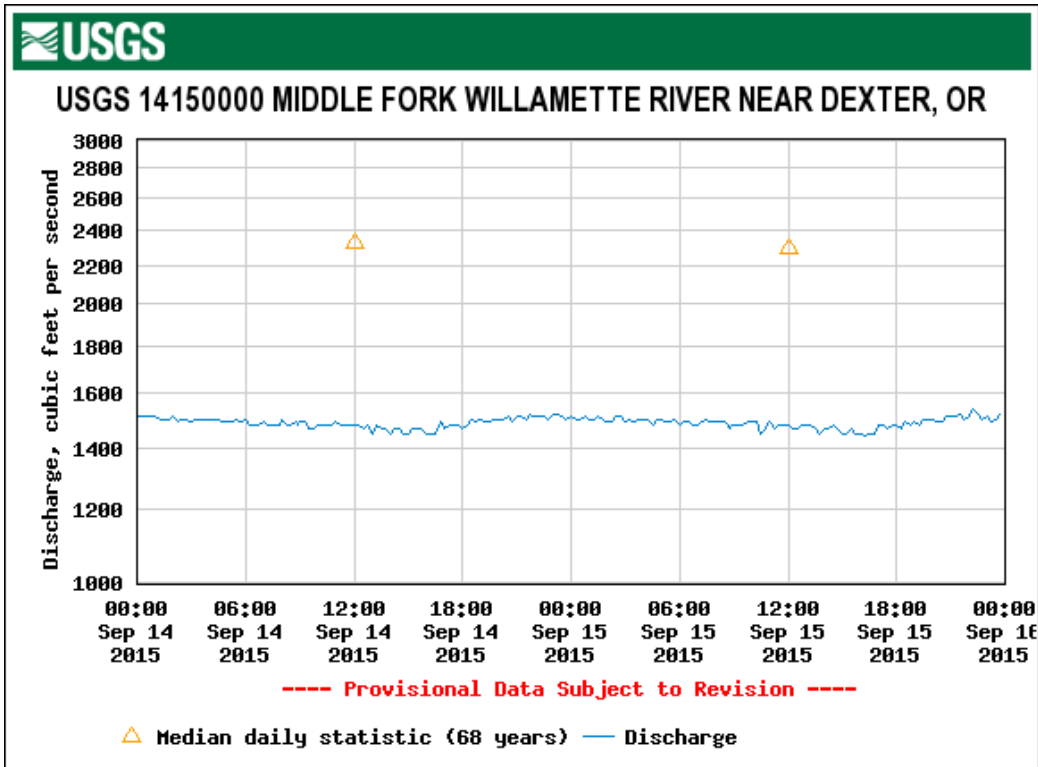


Figure 3: USGS Station 14150000 flow rate along the MF Willamette River near Dexter at the time of LiDAR acquisition.



These photos taken by QSI acquisition staff display water clarity conditions of the MF Willamette River, at the time of LiDAR acquisition.

Airborne LiDAR Survey

The LiDAR survey was accomplished using a Leica ALS80 system dually mounted with a Riegl VQ-820-G topobathymetric sensor in a Cessna Caravan. The Riegl VQ-820-G uses a green wavelength ($\lambda=532$ nm) laser that is capable of collecting high resolution vegetation and topography data, as well as penetrating the water surface with minimal spectral absorption by water. The recorded waveform enables range measurements for all discernible targets for a given pulse. The Leica ALS80 laser system can record unlimited range measurements (returns) per pulse. It is not uncommon for some types of surfaces (e.g., dense vegetation or water) to return fewer pulses to the LiDAR sensor than the laser originally emitted. The discrepancy between first return and overall delivered density will vary depending on terrain, land cover, and the prevalence of water bodies. All discernible laser returns were processed for the output dataset. Table 3 summarizes the settings used to yield an average pulse density of ≥ 4.0 points/m² for green LiDAR returns, and ≥ 8.0 points/m² for NIR LiDAR returns over the Middle Fork Willamette River project area.

Table 3: LiDAR specifications and survey settings

LiDAR Survey Settings & Specifications		
Sensor	Leica ALS80	Riegl VQ-820G
Acquisition Dates	September 14-15, 2015	September 14-15, 2015
Aircraft Used	Cessna Caravan	Cessna Caravan
Survey Altitude (AGL)	400 m	400 m
Target Pulse Rate	495 kHz	284 kHz
Swath Width (m)	323 m	323 m
Pulse Mode	Single Pulse in Air (SPiA)	Single Pulse in Air (SPiA)
Laser Pulse Footprint Diameter	11 cm	40 cm
Field of View	44°	44°
GPS Baselines	≤ 13 nm	≤ 13 nm
GPS PDOP	≤ 3.0	≤ 3.0
GPS Satellite Constellation	≥ 6	≥ 6
Maximum Returns	Unlimited, but typically not more than 5	Unlimited, but typically not more than 7
Intensity	8-bit	16-bit
Resolution/Density	Average 8 pulses/m ²	Average 4 pulses/m ²
Accuracy	RMSE _z ≤ 15 cm	RMSE _z ≤ 15 cm

All areas were surveyed with an opposing flight line side-lap of $\geq 50\%$ ($\geq 100\%$ overlap) in order to reduce laser shadowing and increase surface laser painting. To accurately solve for laser point position (geographic coordinates x, y and z), the positional coordinates of the airborne sensor and the attitude of the aircraft were recorded continuously throughout the LiDAR data collection mission. Position of the aircraft was measured twice per second (2 Hz) by an onboard differential GPS unit, and aircraft attitude was measured 200 times per second (200 Hz) as pitch, roll and yaw (heading) from an onboard inertial measurement unit (IMU). To allow for post-processing correction and calibration, aircraft and sensor position and attitude data are indexed by GPS time.

Ground Control

Ground control surveys, including monumentation and ground survey points (GSPs), were conducted to support the airborne acquisition. Ground control data were used to geospatially correct the aircraft positional coordinate data and to perform quality assurance checks on final LiDAR data.



Previously Existing QSI Monument



Newly-Established QSI Monument

Monumentation

The spatial configuration of ground survey monuments provided redundant control within 13 nautical miles of the mission areas for LiDAR flights. Monuments were also used for collection of ground survey points using real time kinematic (RTK) survey techniques.

Monument locations were selected with consideration for satellite visibility, field crew safety, and optimal location for GSP coverage. QSI utilized two existing monuments and established one new monument for the Middle Fork Willamette River LiDAR project (Table 4, Figure 4). New monumentation was set using 5/8" x 30" rebar topped with stamped 2" aluminum caps. QSI also held coordinates from nearby CORS stations LPSB and OB3C to supplement monument control. QSI's professional land surveyor, Chris Glantz (OR PLS #83648) oversaw and certified the establishment of all monuments.

Table 4: Monuments established for the Middle Fork Willamette River acquisition. Coordinates are on the NAD83 (2011) datum, epoch 2010.00

Monument ID	Latitude	Longitude	Ellipsoid (meters)
LANE_13	44° 00' 41.08475"	-122° 59' 27.48519"	119.047
LANE_15	43° 59' 28.97732"	-122° 56' 10.19436"	139.378
OLC_MFW_01	43° 57' 13.10667"	-122° 45' 45.81019"	215.486

To correct the continuously recorded onboard measurements of the aircraft position, QSI concurrently conducted multiple static Global Navigation Satellite System (GNSS) ground surveys (1 Hz recording frequency) over each monument. During post-processing, the static GPS data were triangulated with nearby Continuously Operating Reference Stations (CORS) using the Online Positioning User Service (OPUS¹) for precise positioning. Multiple independent sessions over the same monument were processed to confirm antenna height measurements and to refine position accuracy.

Monuments were established according to the national standard for geodetic control networks, as specified in the Federal Geographic Data Committee (FGDC) Geospatial Positioning Accuracy Standards

¹ OPUS is a free service provided by the National Geodetic Survey to process corrected monument positions.
<http://www.ngs.noaa.gov/OPUS>.

for geodetic networks.² This standard provides guidelines for classification of monument quality at the 95% confidence interval as a basis for comparing the quality of one control network to another. The monument rating for this project is shown in Table 5.

Table 5: Federal Geographic Data Committee monument rating for network accuracy

Direction	Rating
1.96 * St Dev _{NE} :	0.020 m
1.96 * St Dev _z :	0.050 m

For the Middle Fork Willamette River LiDAR project, the monument coordinates contributed no more than 5.4 cm of positional error to the geolocation of the final ground survey points and LiDAR, with 95% confidence.

Ground Survey Points (GSPs)

Ground survey points were collected using real time kinematic survey techniques. A Trimble R7 base unit was positioned at a nearby monument to broadcast a kinematic correction to a roving Trimble R10 GNSS receiver. All GSP measurements were made during periods with a Position Dilution of Precision (PDOP) of ≤ 3.0 with at least six satellites in view of the stationary and roving receivers. When collecting RTK data, the rover records data while stationary for five seconds, then calculates the pseudorange position using at least three one-second epochs. Relative errors for any GSP position must be less than 1.5 cm horizontal and 2.0 cm vertical in order to be accepted. See Table 6 for Trimble unit specifications.

GSPs were collected in areas where good satellite visibility was achieved on paved roads and other hard surfaces such as gravel or packed dirt roads. GSP measurements were not taken on highly reflective surfaces such as center line stripes or lane markings on roads due to the increased noise seen in the laser returns over these surfaces. GSPs were collected within as many flightlines as possible; however the distribution of GSPs depended on ground access constraints and monument locations and may not be equitably distributed throughout the study area (Figure 4).

Table 6: Trimble equipment identification

Receiver Model	Antenna	OPUS Antenna ID	Use
Trimble R7 GNSS	Zephyr GNSS Geodetic Model 2 RoHS	TRM57971.00	Static
Trimble R10	Integrated Antenna R10	TRMR10	Static, Rover

² Federal Geographic Data Committee, Geospatial Positioning Accuracy Standards (FGDC-STD-007.2-1998). Part 2: Standards for Geodetic Networks, Table 2.1, page 2-3. <http://www.fgdc.gov/standards/projects/FGDC-standards-projects/accuracy/part2/chapter2>

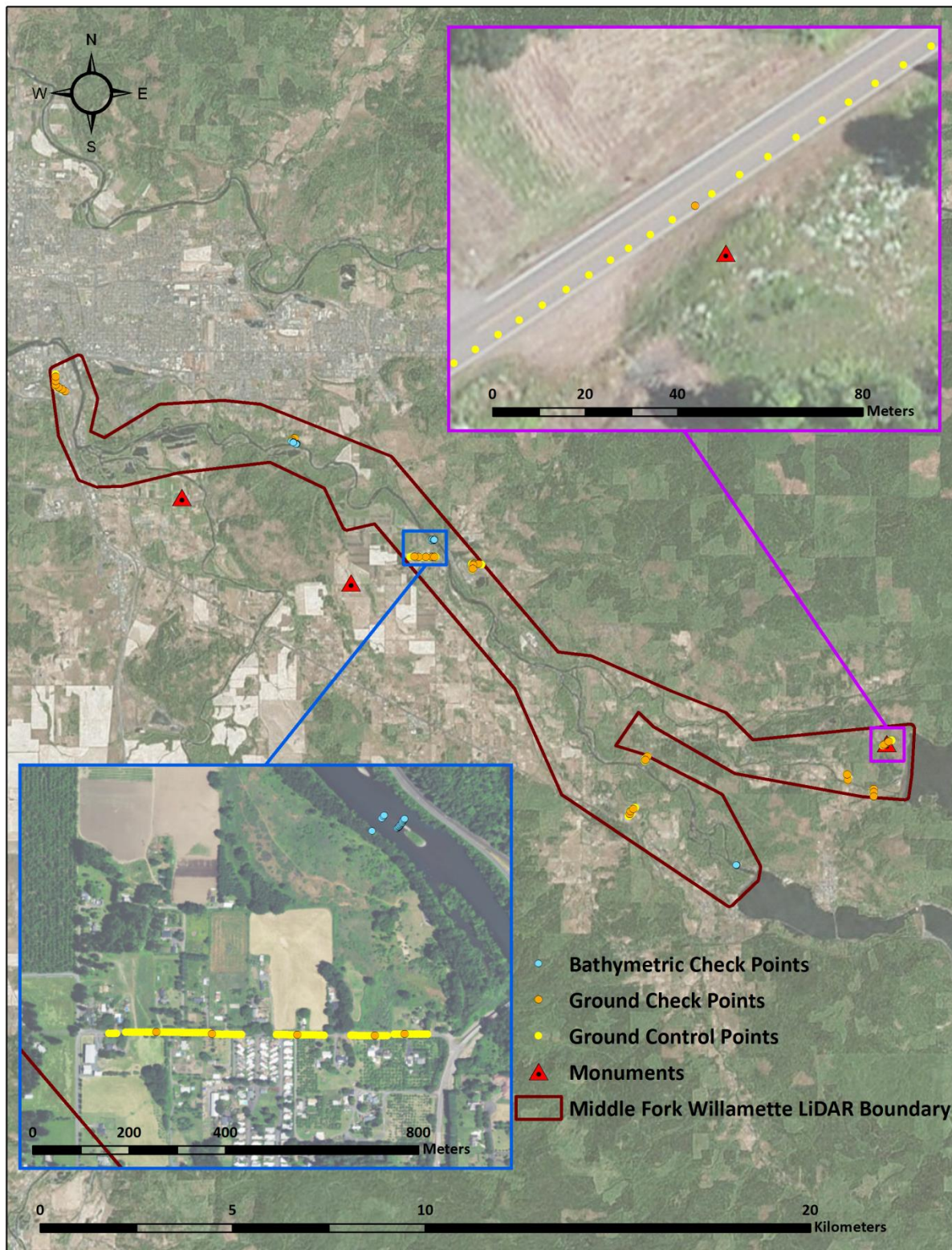


Figure 4: Ground survey location map

■ Ground
■ Default
■ Bathymetric Surface
■ Water Column

This 3 meter LiDAR cross section shows bank edge vegetation and bathymetric bottom returns.

Topobathymetric LiDAR Data

Upon completion of data acquisition, QSI processing staff initiated a suite of automated and manual techniques to process the data into the requested deliverables. Processing tasks included GPS control computations, smoothed best estimate trajectory (SBET) calculations, kinematic corrections, calculation of laser point position, sensor and data calibration for optimal relative and absolute accuracy, and LiDAR point classification (Table 7). Riegl's RiProcess software was used to facilitate bathymetric return processing. Once bathymetric points were differentiated, they were spatially corrected for refraction through the water column based on the angle of incidence of the laser. QSI refracted water column points using QSI's proprietary LAS processing software, LAS Monkey. The resulting point cloud data were classified using both manual and automated techniques. Processing methodologies were tailored for the landscape. Brief descriptions of these tasks are shown in Table 8.

Table 7: ASPRS LAS classification standards applied to the Middle Fork Willamette River dataset

Classification Number	Classification Name	Classification Description
1	Default/Unclassified	Laser returns that are not included in the ground class, composed of vegetation and man-made structures
2	Ground	Laser returns that are determined to be ground using automated and manual cleaning algorithms
9	Water	Laser returns that are determined to be water surface using automated and manual cleaning algorithms

Classification Number	Classification Name	Classification Description
25	Water Column	Refracted Riegl sensor returns that are determined to be water using automated and manual cleaning algorithms.
26	Bathymetric Bottom	Refracted Riegl sensor returns that fall within the water's edge breakline which characterize the submerged topography.

Table 8: LiDAR processing workflow

LiDAR Processing Step	Software Used
Resolve kinematic corrections for aircraft position data using kinematic aircraft GPS and static ground GPS data. Develop a smoothed best estimate of trajectory (SBET) file that blends post-processed aircraft position with sensor head position and attitude recorded throughout the survey.	Waypoint Inertial Explorer v.8.6 Applanix PosPac v.6.2
Calculate laser point position by associating SBET position to each laser point return time, scan angle, intensity, etc. Create raw laser point cloud data for the entire survey in *.las (ASPRS v. 1.2) format. Convert data to orthometric elevations by applying a geoid12a correction.	RiProcess v1.6.4 Waypoint Inertial Explorer v.8.6 Leica Cloudpro v. 1.2.1 TerraMatch v.15
Import raw laser points into manageable blocks (less than 500 MB) to perform manual relative accuracy calibration and filter erroneous points. Classify ground points for individual flight lines.	TerraScan v.15
Using ground classified points per each flight line, test the relative accuracy. Perform automated line-to-line calibrations for system attitude parameters (pitch, roll, heading), mirror flex (scale) and GPS/IMU drift. Calculate calibrations on ground classified points from paired flight lines and apply results to all points in a flight line. Use every flight line for relative accuracy calibration.	TerraMatch v.15 RiProcess v1.6.4
Apply refraction correction to all subsurface returns.	LAS Monkey (QSI)
Classify resulting data to ground and other client designated ASPRS classifications (Table 7). Assess statistical absolute accuracy via direct comparisons of ground classified points to ground control survey data.	TerraScan v.15 TerraModeler v.15
Generate bare earth models as triangulated surfaces. Generate highest hit models as a surface expression of all classified points. Export all surface models as ESRI GRIDs at a 1 meter pixel resolution.	TerraScan v.15 TerraModeler v.15 ArcMap v. 10.1
Export intensity images as GeoTIFFs at a 0.5 meter pixel resolution.	DZ Ortho Creator (QSI)

Bathymetric Refraction

The water surface model used for refraction is generated using NIR points within the breaklines defining the water's edge. Points are filtered and edited to obtain the most accurate representation of the water surface and are used to create a water surface model TIN. A tin model is preferable to a raster based water surface model to obtain the most accurate angle of incidence during refraction. The refraction processing is done using Las Monkey; QSI's proprietary LiDAR processing tool. After refraction, the points are compared against bathymetric control points to assess accuracy.

LiDAR Derived Products

Because hydrographic laser scanners penetrate the water surface to map submerged topography, this affects how the data should be processed and presented in derived products from the LiDAR point cloud. The following discusses certain derived products that vary from the traditional (NIR) specification and delivery format.

Topobathymetric DEMs

Bathymetric bottom returns can be limited by depth, water clarity, and bottom surface reflectivity. Water clarity and turbidity affects the depth penetration capability of the green wavelength laser with returning laser energy diminishing by scattering throughout the water column. Additionally, the bottom surface must be reflective enough to return remaining laser energy back to the sensor at a detectable level. Although the predicted depth penetration range of the Riegl VQ-820-G sensor is one Secchi depth on brightly reflective surfaces, it is not unexpected to have no bathymetric bottom returns in turbid or non-reflective areas.

As a result, creating digital elevation models (DEMs) presents a challenge with respect to interpolation of areas with no returns. Traditional DEMs are "unclipped", meaning areas lacking ground returns are interpolated from neighboring ground returns (or breaklines in the case of hydro-flattening), with the assumption that the interpolation is close to reality. In bathymetric modeling, these assumptions are prone to error because a lack of bathymetric returns can indicate a change in elevation that the laser can no longer map due to increased depths. The resulting void areas may suggest greater depths, rather than similar elevations from neighboring bathymetric bottom returns. Therefore, QSI created a water polygon with bathymetric coverage to delineate areas with successfully mapped bathymetry. This shapefile was used to control the extent of the delivered clipped topobathymetric model to avoid false triangulation (interpolation from TIN'ing) across areas in the water with no bathymetric returns.

Intensity Images

In traditional NIR LiDAR, intensity images are often made using first return information. For bathymetric LiDAR however, it is most often the last returns that capture features of interest below the water's surface. Therefore, a first return intensity image would display intensity information of the water's surface, obscuring the features of interest below.

With bathymetric LiDAR a more detailed and informative intensity image can be created by using all or selected point classes, rather than relying on return number alone. If intensity information of the bathymetry is the primary goal, water surface and water column points can be excluded. However, water surface and water column points often contain potentially useful information about turbidity and submerged but unclassified features such as vegetation. For the Middle Fork Willamette River project, QSI created one set of intensity images from NIR laser first returns, as well as one set of intensity images

from green laser returns. Green laser intensity images were created using first returns over terrestrial areas only, as well as all water column and bathymetric bottom points in order to display more detail in intensity values (Figure 5).

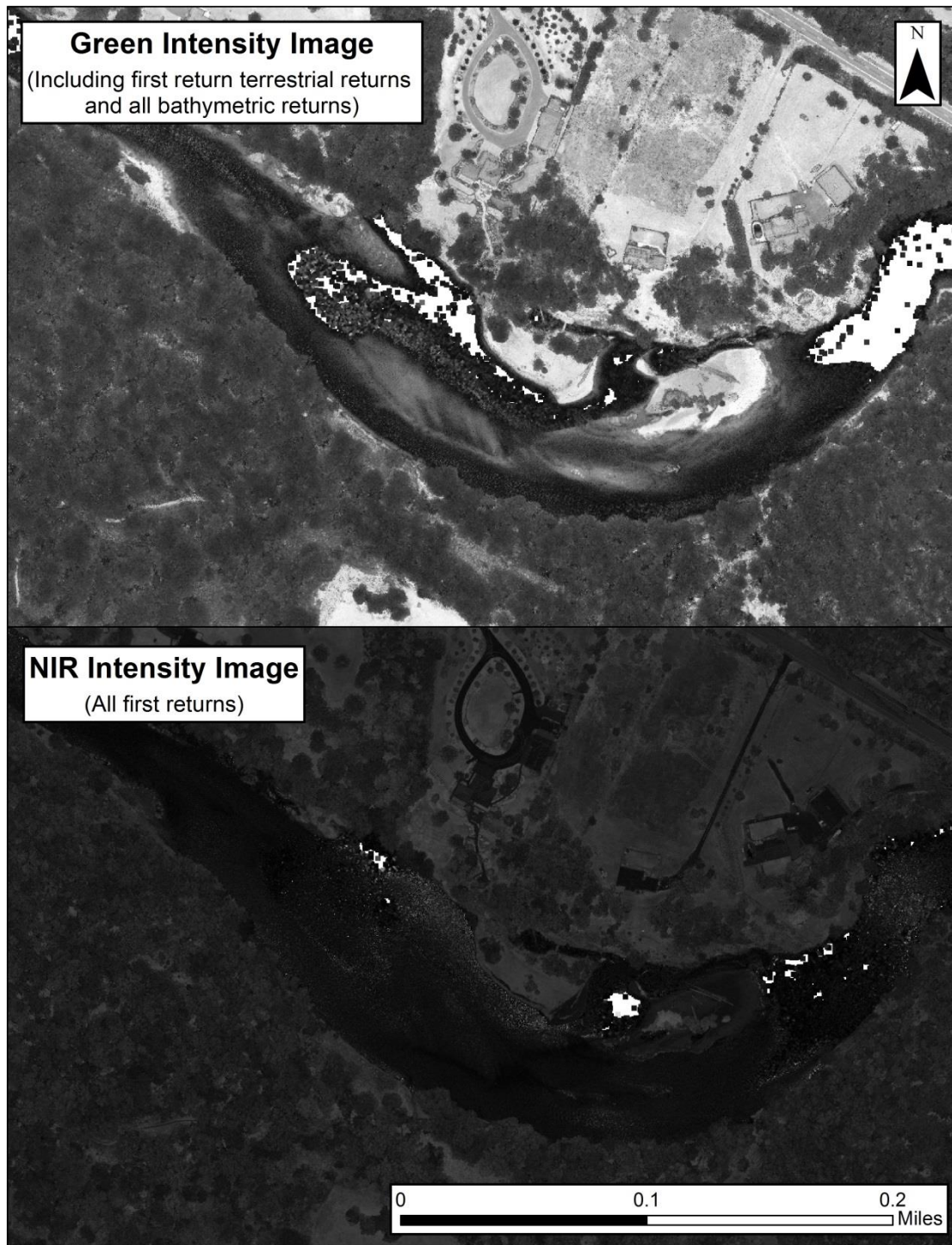
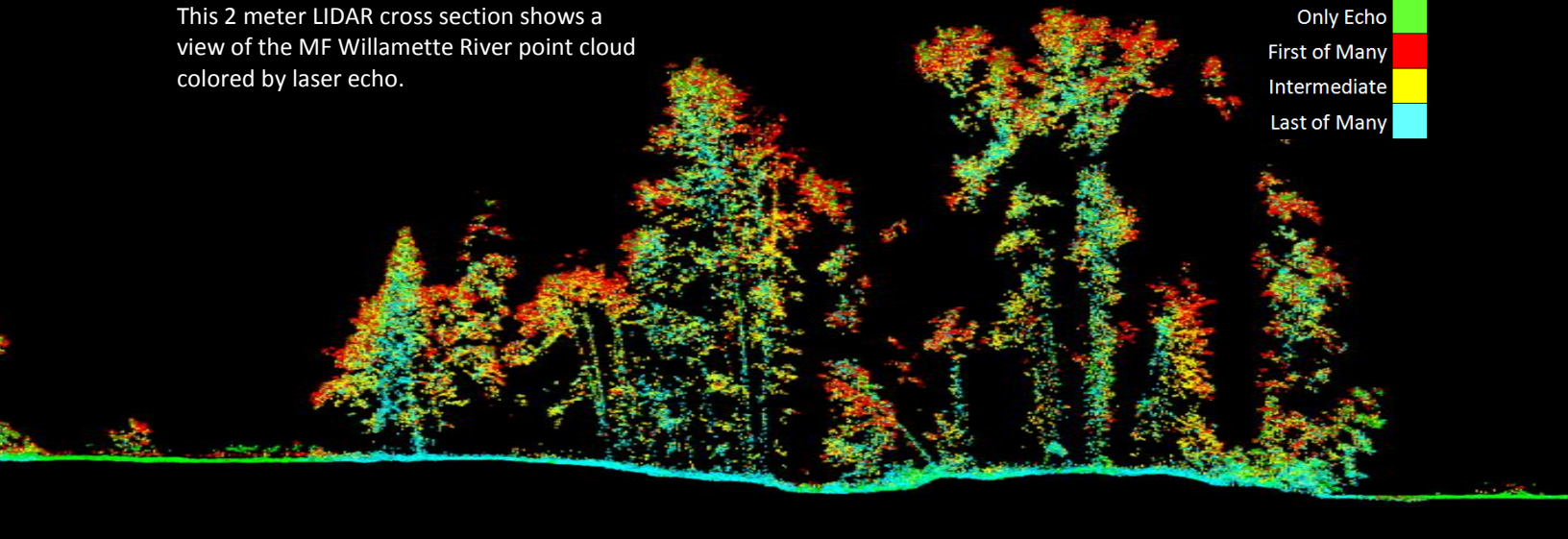


Figure 5: A comparison of Intensity Images from Green and NIR returns in the Middle Fork Willamette River area

This 2 meter LIDAR cross section shows a view of the MF Willamette River point cloud colored by laser echo.

Only Echo
First of Many
Intermediate
Last of Many



Bathymetric LiDAR

An underlying principle for collecting hydrographic LiDAR data is to survey near-shore areas that can be difficult to collect with other methods, such as multi-beam sonar, particularly over large areas. In order to determine the capability and effectiveness of the bathymetric LiDAR, several parameters were considered; depth penetrations below the water surface, bathymetric return density, and spatial accuracy.

Mapped Bathymetry and Depth Penetration

The specified depth penetration range of the Riegl VQ-820-G sensor is one secchi depth; therefore, bathymetry data below one secchi depth at the time of acquisition is not to be expected. To assist in evaluating performance results of the sensor, a polygon layer was created to delineate areas where bathymetry was successfully mapped.

This shapefile was used to control the extent of the delivered clipped topo-bathymetric model and to avoid false triangulation across areas in the water with no returns. Insufficiently mapped areas were identified by triangulating bathymetric bottom points with an edge length maximum of 4.56 meters. This ensured all areas of no returns ($> 9 \text{ m}^2$), were identified as data voids. Of the areas successfully mapped, 46.50% had a calculated depth of 0 – 0.5m, 38.00% had a calculated depth of 0.51 -1.0 m, 13.89% had a calculated depth of 1.01 – 1.5m, and the remaining 1.61% had a calculated depth between 1.51m and 6.5m (Table 9).

Confidence

In bathymetric LiDAR collection, there are generally fewer returns at greater depths and uncertainty exists as to whether the return is actually a bottom return or part of the water column. In order to more closely assess the depths mapped, bathymetric point density was considered. The distribution of the point density within the mapped area varied depending on depth. Confidence in bathymetric elevation data was assessed by looking at average point density within an area of 9m^2 radiating out from the center of any given 1 meter cell ($r = 1.69\text{ m}$). If the 9m^2 search area around the 1 m cell had an average point density of $\leq 1\text{ point/m}^2$, the cell was considered an area of low confidence due to a lack of surrounding data to confirm bathymetric elevations. Cells whose search area had an average point density of $\geq 1\text{m}^2$ were considered adequately covered with high confidence in the bathymetric data elevations represented (Figure 6). Of the successfully mapped areas, 93.58% were mapped with high confidence and 6.42% were considered low confidence (Figure 7, Table 9). The confidence attribute within the mapped area shapefile provided was created based on this information. It should be noted that confidence levels are designed for assessing the overall model of topography at a spatial resolution of 1m^2 .

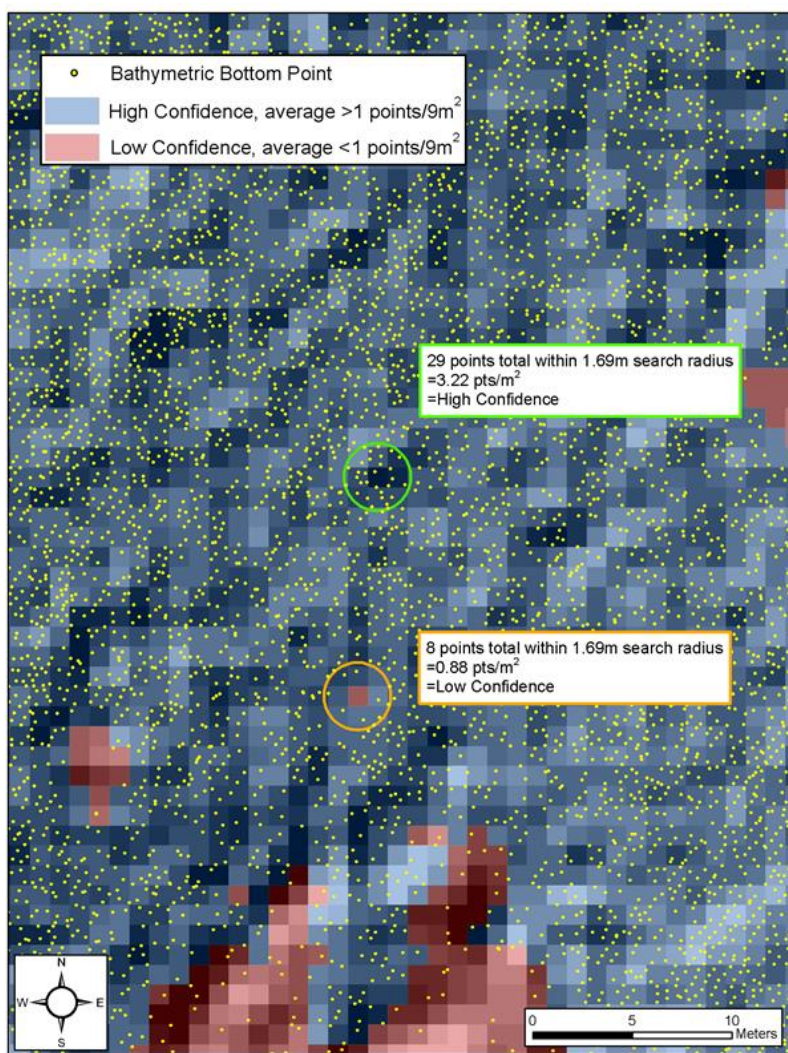


Figure 6: Sample plot of low and high confidence in bathymetric returns

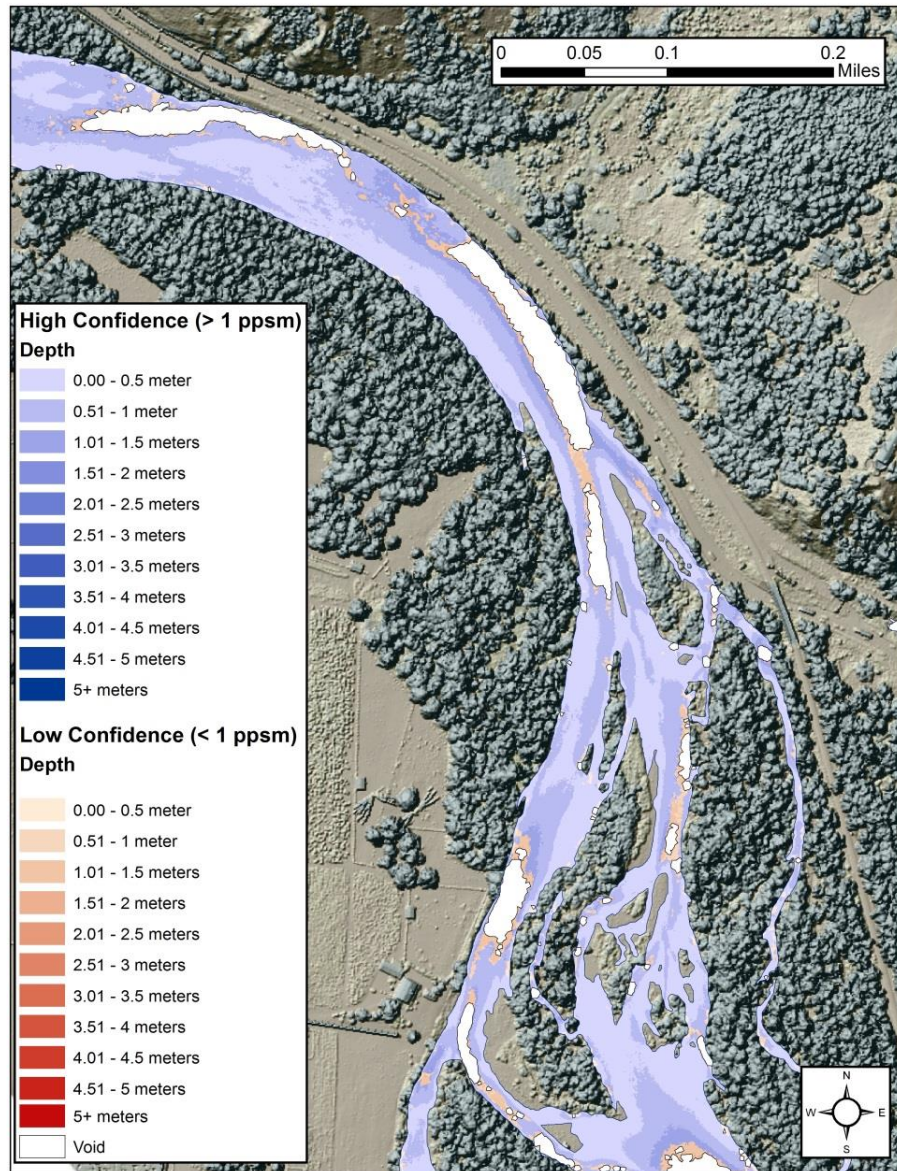


Figure 7: Sample image from the Middle Fork Willamette River project showing confidence values and data voids

Table 9: Percentage of successfully mapped bathymetry by depth and confidence

Depth Range	Percentage of Successfully Mapped Areas	Percentage Identified as High Confidence	Percentage Identified as Low Confidence
0.00 – 0.50 m	46.50 %	97.11 %	2.89 %
0.51 – 1.00 m	38.00 %	97.05 %	2.95 %
1.01 – 1.50 m	13.89 %	77.32 %	22.68 %
1.51 – 6.5 m	1.61 %	50.03 %	49.97 %

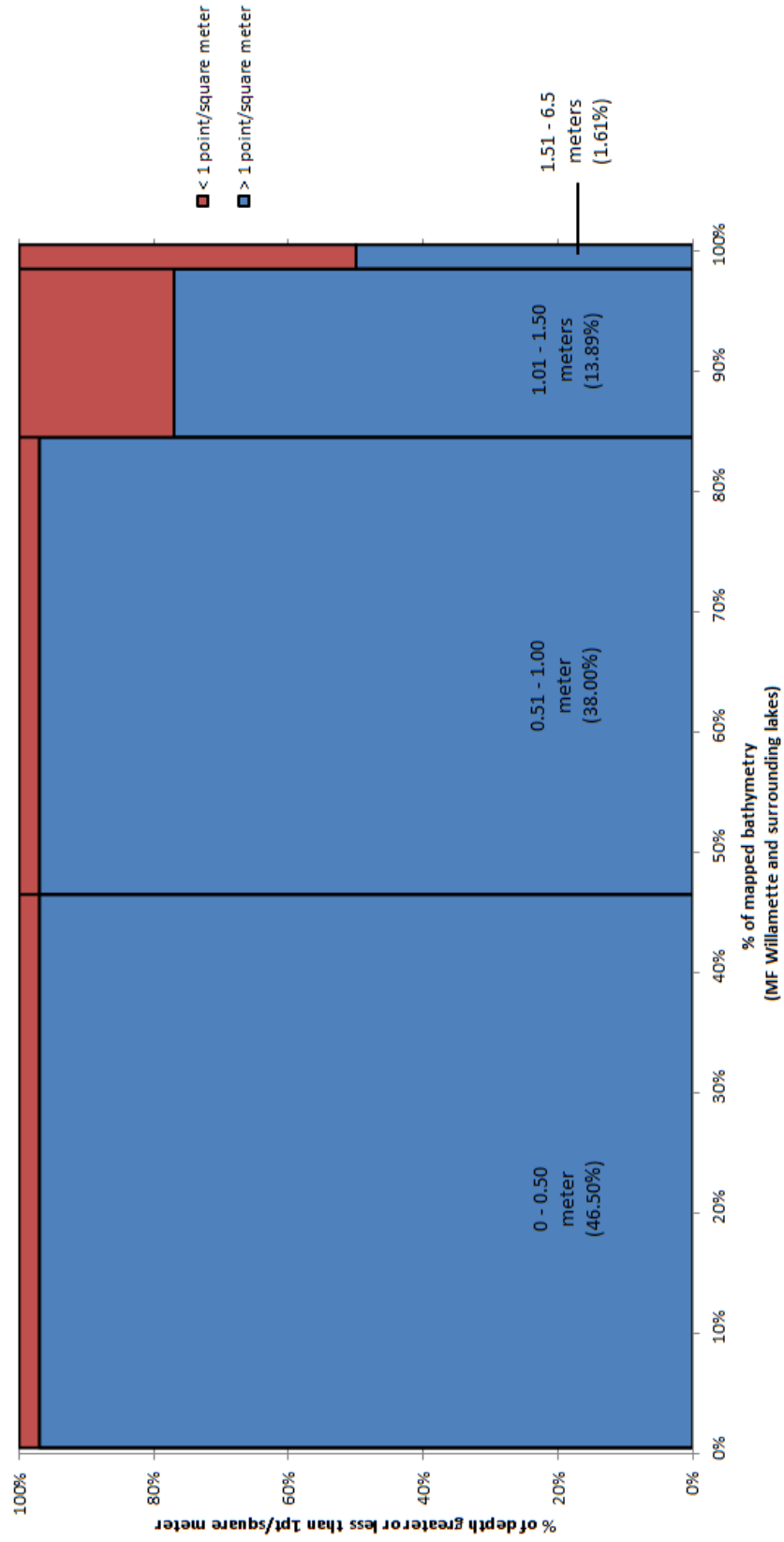


Figure 8: Depth percentages and point density by depth percentages for the Middle Fork Willamette River project

LiDAR Point Density

First Return Point Density

The acquisition parameters were designed to acquire an average first-return density of 4 points/m² for the topo-bathymetric returns, and 6 points/m² for the NIR returns. First return density describes the density of pulses emitted from the laser that return at least one echo to the system. Multiple returns from a single pulse were not considered in first return density analysis. Some types of surfaces (e.g., breaks in terrain, water and steep slopes) may have returned fewer pulses than originally emitted by the laser.

With NIR LiDAR, first returns typically reflect off the highest feature on the landscape within the footprint of the pulse. In forested or urban areas the highest feature could be a tree, building or power line, while in areas of unobstructed ground, the first return will be the only echo and represents the bare earth surface.

The average first-return density of the green wavelength LiDAR data for the Middle Fork Willamette River project was 18.42 points/m² while the average first-return density of the NIR wavelength LiDAR data was 61.47 points/m². Cumulatively, the average first return density was 79.89 points/m². The statistical and spatial distributions of all first return densities per 100 m x 100 m cell are portrayed in Figure 9 through Figure 12.

Table 10: Average First Return LiDAR point densities

First Return Type	Point Density
Green Sensor First Returns	18.42 points/m ²
NIR Sensor First Returns	61.47 points/m ²
Cumulative Integrated First Returns	79.89 points/m ²

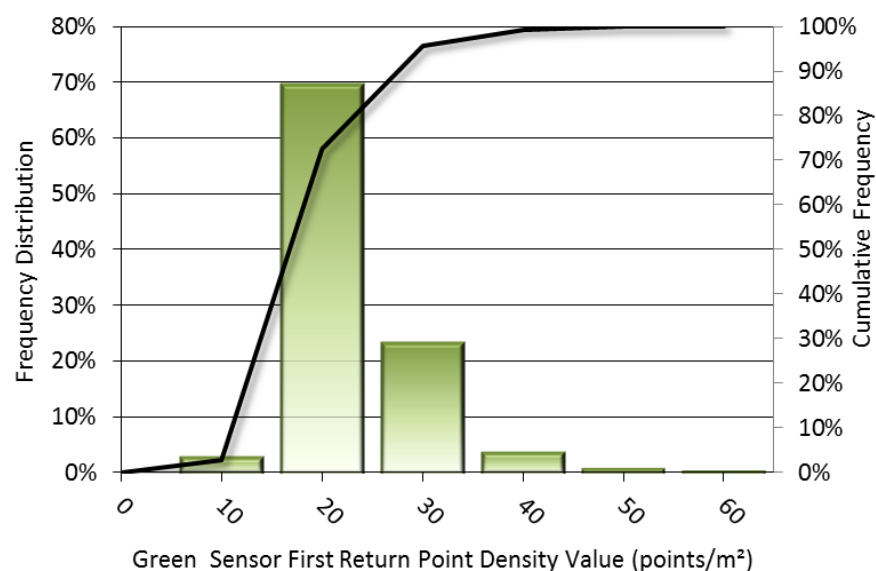


Figure 9: Frequency distribution of green sensor first return densities per 100 x 100 m cell

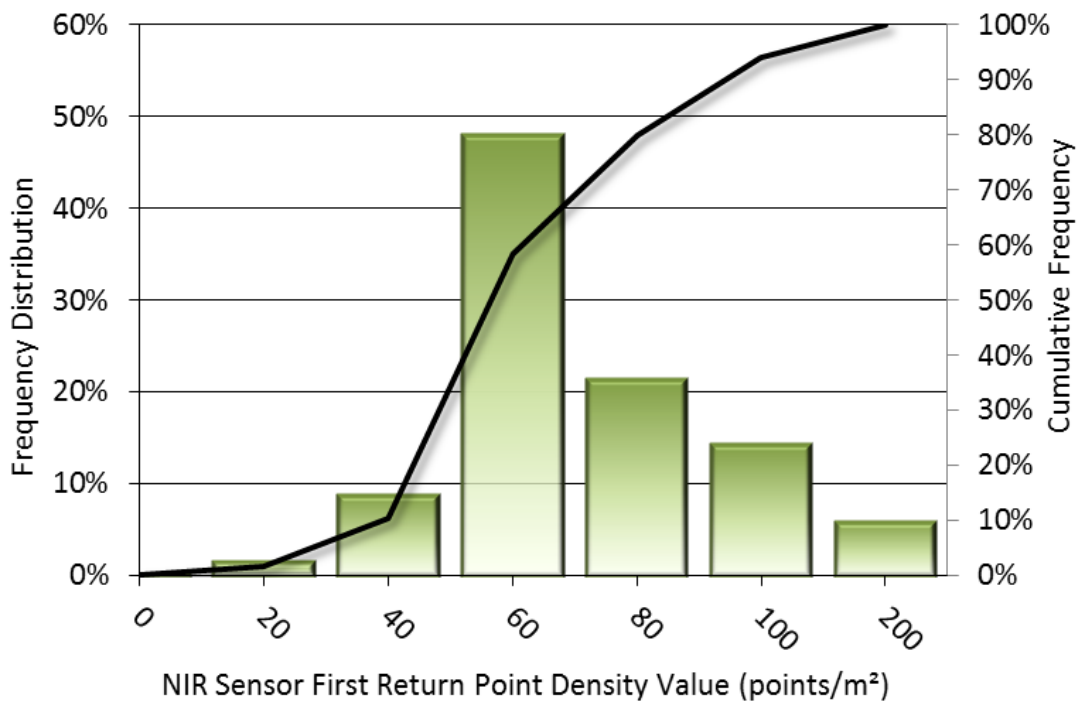


Figure 10: Frequency distribution of NIR sensor first return densities per 100 x 100 m cell

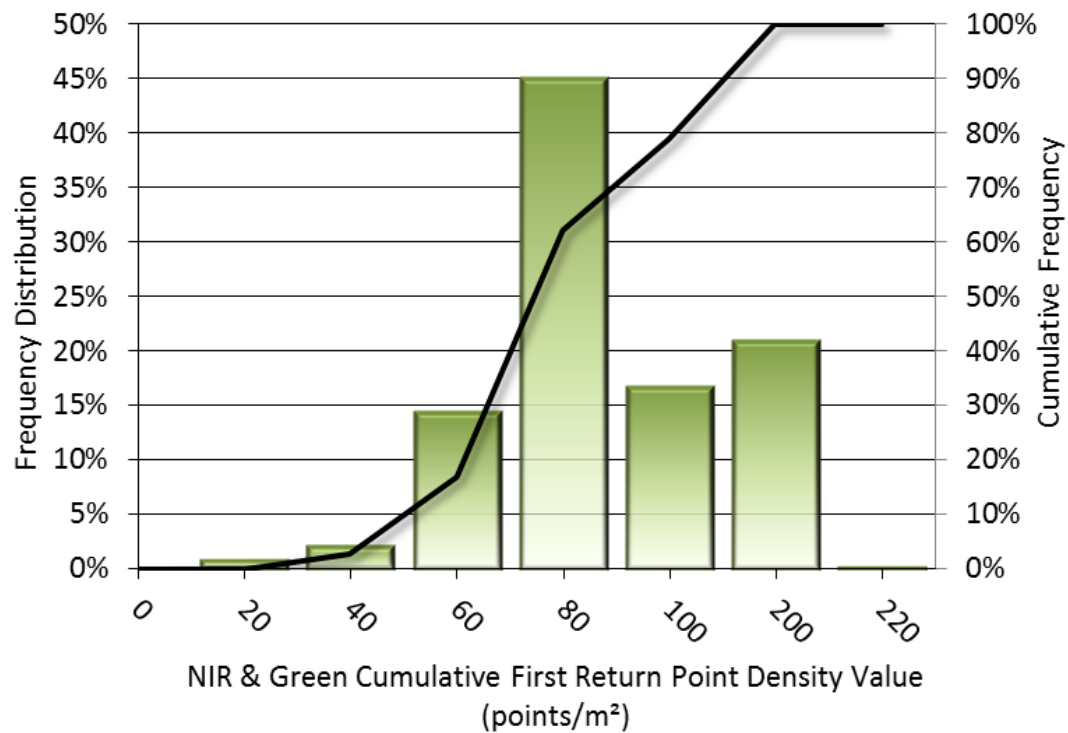


Figure 11: Frequency distribution of cumulative first return densities per 100 x 100 m cell



Figure 12: First return density map by sensor for the Middle Fork Willamette River site (100 m x 100 m cells)

Bathymetric and Ground Classified Point Densities

The density of ground classified LiDAR returns and bathymetric bottom returns were also analyzed for this project. Terrain character, land cover, and ground surface reflectivity all influenced the density of ground surface returns. In vegetated areas, fewer pulses may have penetrated the canopy, resulting in lower ground density. Similarly, the density of bathymetric bottom returns was influenced by turbidity, depth, and bottom surface reflectivity. In turbid areas, fewer pulses may have penetrated the water surface, resulting in lower bathymetric density.

The ground and bathymetric bottom classified density of LiDAR data for the Middle Fork Willamette River project was 11.24 points/m² (Table 11). The statistical and spatial distributions ground classified and bathymetric bottom return densities per 100 m x 100 m cell are portrayed in Figure 13 and Figure 14.

Additionally, for the Middle Fork Willamette River project, density values of only bathymetric bottom returns were calculated for all areas considered mapped. Areas lacking bathymetric returns (voids, see Figure 7) were not considered in calculating an average density value. Within the successfully mapped area, a bathymetric bottom return density of 5.65 points/m² was achieved.

Table 11: Average Ground and Bathymetric Classified LiDAR point densities

Classification	Point Density
Ground and Bathymetric Bottom Classified Returns	11.24 points/m ²

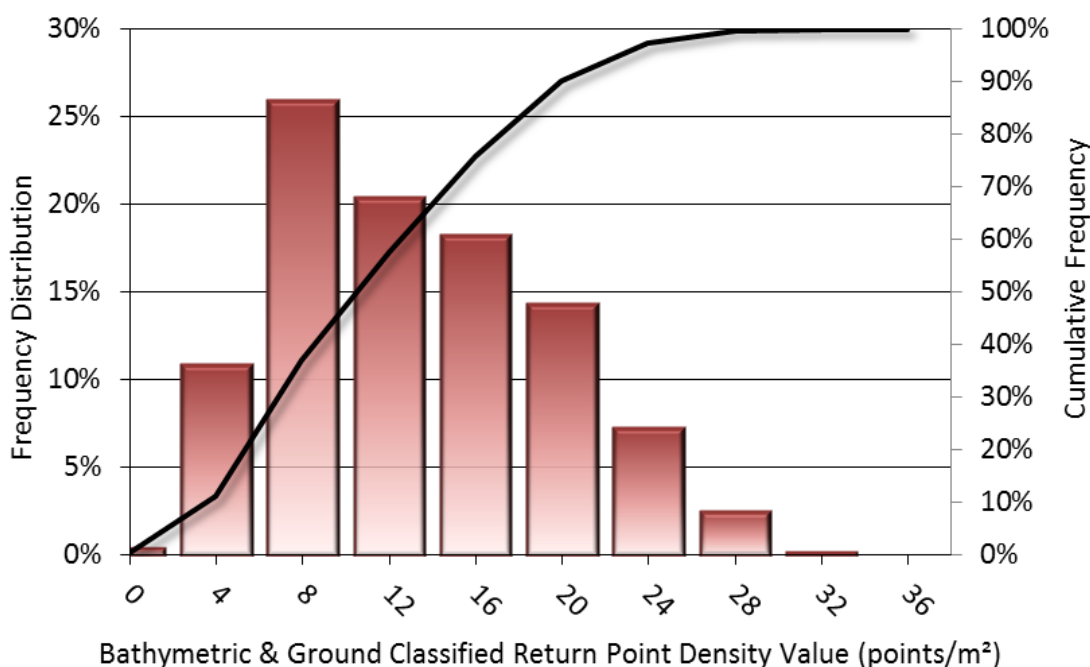


Figure 13: Frequency distribution of bathymetric and ground classified return densities per 100 x 100 m cell

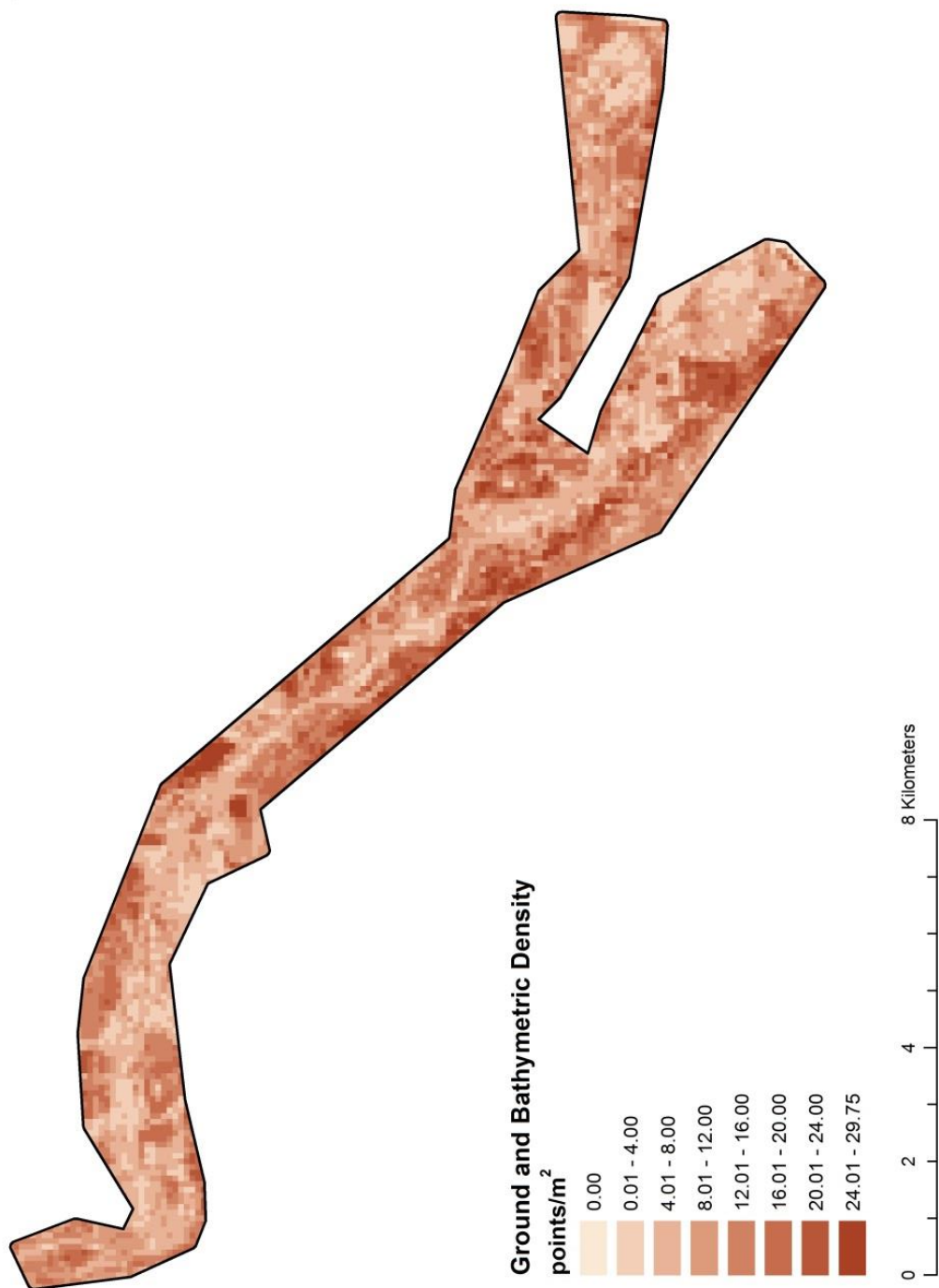


Figure 14: Ground density and cumulative first return map for the Middle Fork Willamette River site (100 m x 100 m cells)

LiDAR Accuracy Assessments

The accuracy of the LiDAR data collection can be described in terms of absolute accuracy (the consistency of the data with external data sources) and relative accuracy (the consistency of the dataset with itself). See Appendix A for further information on sources of error and operational measures used to improve relative accuracy.

LiDAR Absolute Accuracy

Absolute accuracy was assessed using Fundamental Vertical Accuracy (FVA) reporting designed to meet guidelines presented in the FGDC National Standard for Spatial Data Accuracy³. FVA compares known ground check point data collected on open, bare earth surfaces with level slope (<20°) to the triangulated surface generated by the LiDAR points. FVA is a measure of the accuracy of LiDAR point data in open areas where the LiDAR system has a high probability of measuring the ground surface and is evaluated at the 95% confidence interval ($1.96 * RMSE$), as shown in Table 12.

The mean and standard deviation (σ) of divergence of the ground surface model from ground check point coordinates are also considered during accuracy assessment. These statistics assume the error for x, y and z is normally distributed, and therefore the skew and kurtosis of distributions are also considered when evaluating error statistics. For the Middle Fork Willamette River survey, 30 ground check points were withheld in total resulting in a fundamental vertical accuracy of 0.060 meters (Figure 15). Additionally, 45 bathymetric (submerged or along the water's edge) check points were also collected in order to assess the submerged surface vertical accuracy, resulting in an average absolute accuracy of 0.012 meters (Table 12).

QSI also assessed absolute accuracy using 555 ground control points. Although these points were used in the calibration and post-processing of the LiDAR point cloud, they may still provide a good indication of the overall accuracy of the LiDAR dataset, and therefore have been provided in Table 12 and Figure 17.

Table 12: Absolute accuracy results

	Absolute Accuracy		
	Ground Check Points (FVA)	Bathymetric Check Points	Ground Control Points
Sample	30 points	45 points	555 points
FVA ($1.96 * RMSE$)	0.060 m	0.072 m	0.055 m
Average	0.000 m	0.012 m	-0.003 m
Median	0.002 m	0.010 m	-0.001 m
RMSE	0.031 m	0.037 m	0.028 m
Standard Deviation (1σ)	0.031 m	0.035 m	0.028 m

³ Federal Geographic Data Committee, Geospatial Positioning Accuracy Standards (FGDC-STD-007.3-1998). Part 3: National Standard for Spatial Data Accuracy. <http://www.fgdc.gov/standards/projects/FGDC-standards-projects/accuracy/part3/chapter3>

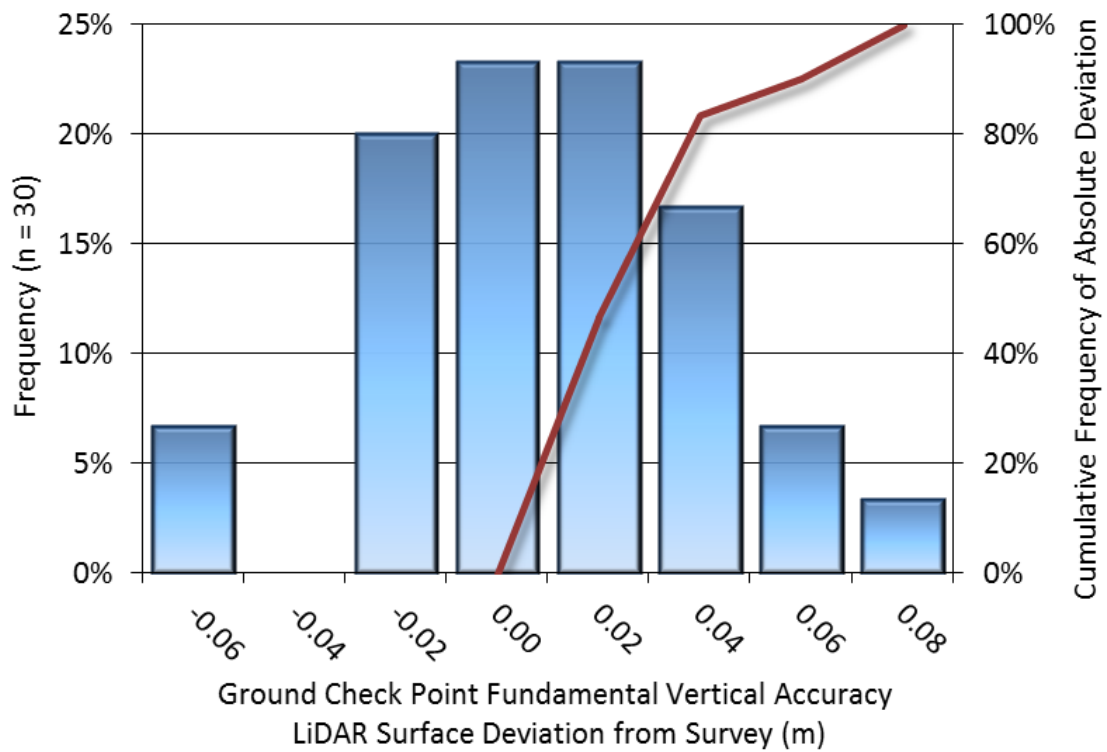


Figure 15: Frequency histogram for LiDAR surface deviation from ground check point values

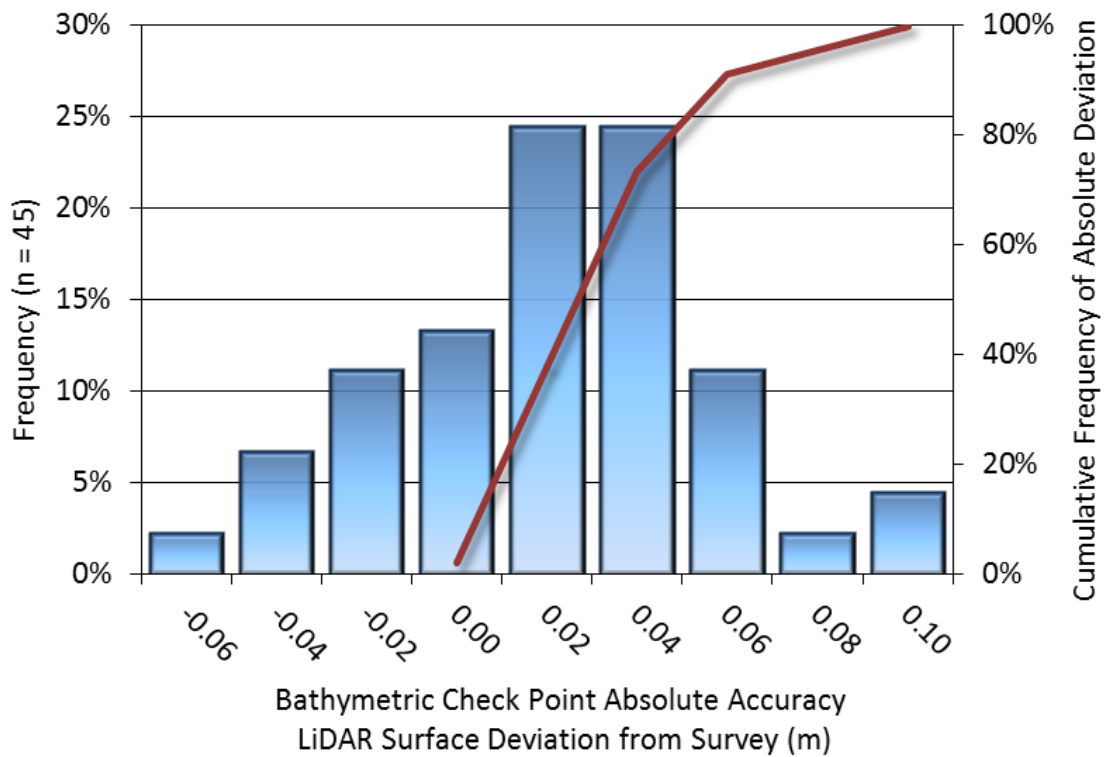


Figure 16: Frequency histogram for LiDAR surface deviation from bathymetric check point values

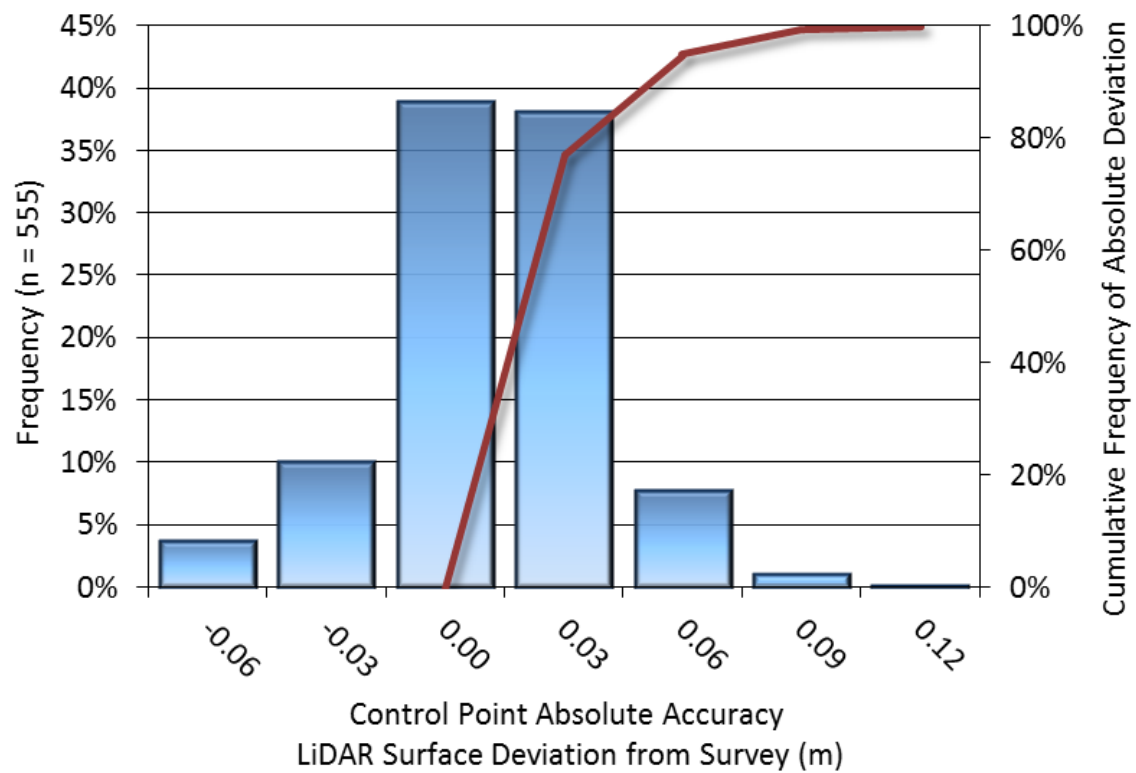


Figure 17: Frequency histogram for LiDAR surface deviation from ground control point values

LiDAR Relative Vertical Accuracy

Relative vertical accuracy refers to the internal consistency of the data set as a whole: the ability to place an object in the same location given multiple flight lines, GPS conditions, and aircraft attitudes. When the LiDAR system is well calibrated, the swath-to-swath vertical divergence is low (<0.10 meters). The relative vertical accuracy was computed by comparing the ground surface model of each individual flight line with its neighbors in overlapping regions. The average (mean) line to line relative vertical accuracy for the Middle Fork Willamette River LiDAR project is 0.032 meters (Table 13, Figure 18).

Table 13: Relative accuracy results

Relative Accuracy	
Sample	175 surfaces
Average	0.032 m
Median	0.032 m
RMSE	0.034 m
Standard Deviation (1σ)	0.008 m
1.96 σ	0.016 m

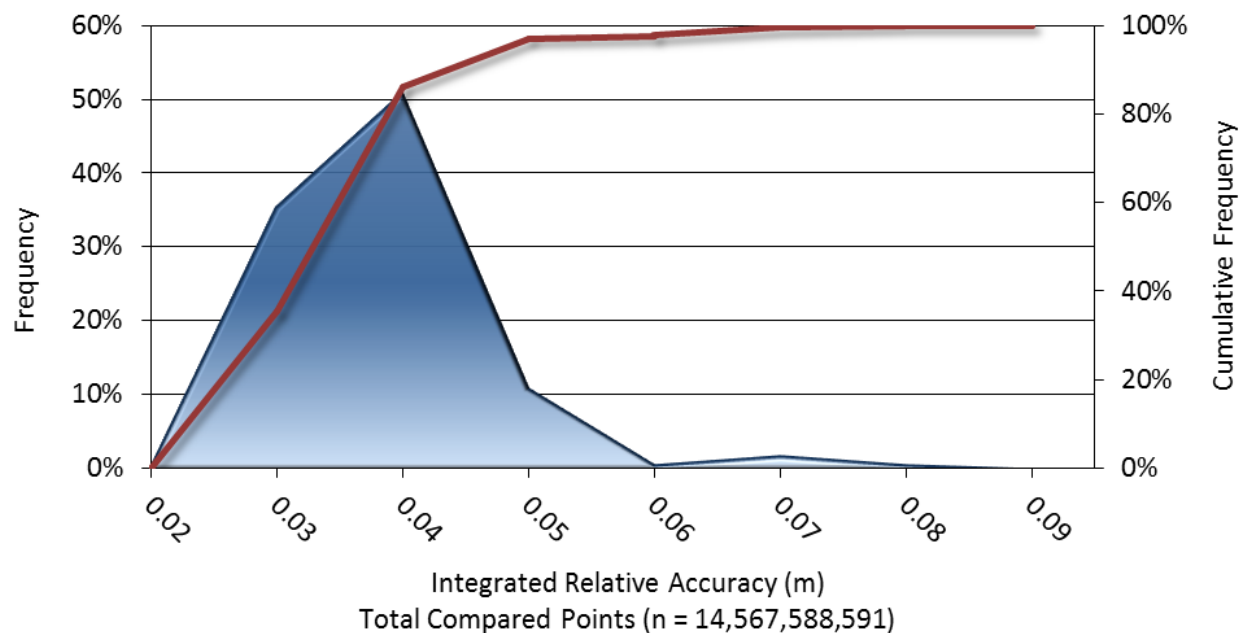


Figure 18: Frequency plot for relative vertical accuracy between flight lines

CERTIFICATIONS

Quantum Spatial provided LiDAR services for the OLC Middle Fork Willamette River LiDAR project as described in this report.

I, Christopher Glantz, being duly registered as a Professional Land Surveyor in and by the state of Oregon, hereby certify that the methodologies, static GNSS occupations used during airborne flights, and ground survey point collection were performed using commonly accepted Standard Practices. Field work conducted for this report was between September 14, 2015 and September 16, 2015.

Accuracy statistics shown in the Accuracy Section of this Report have been reviewed by me and found to meet the "National Standard for Spatial Data Accuracy".



1/22/2016

Christopher Glantz, PLS
Land Survey Manager
Quantum Spatial, Inc.



SELECTED IMAGES

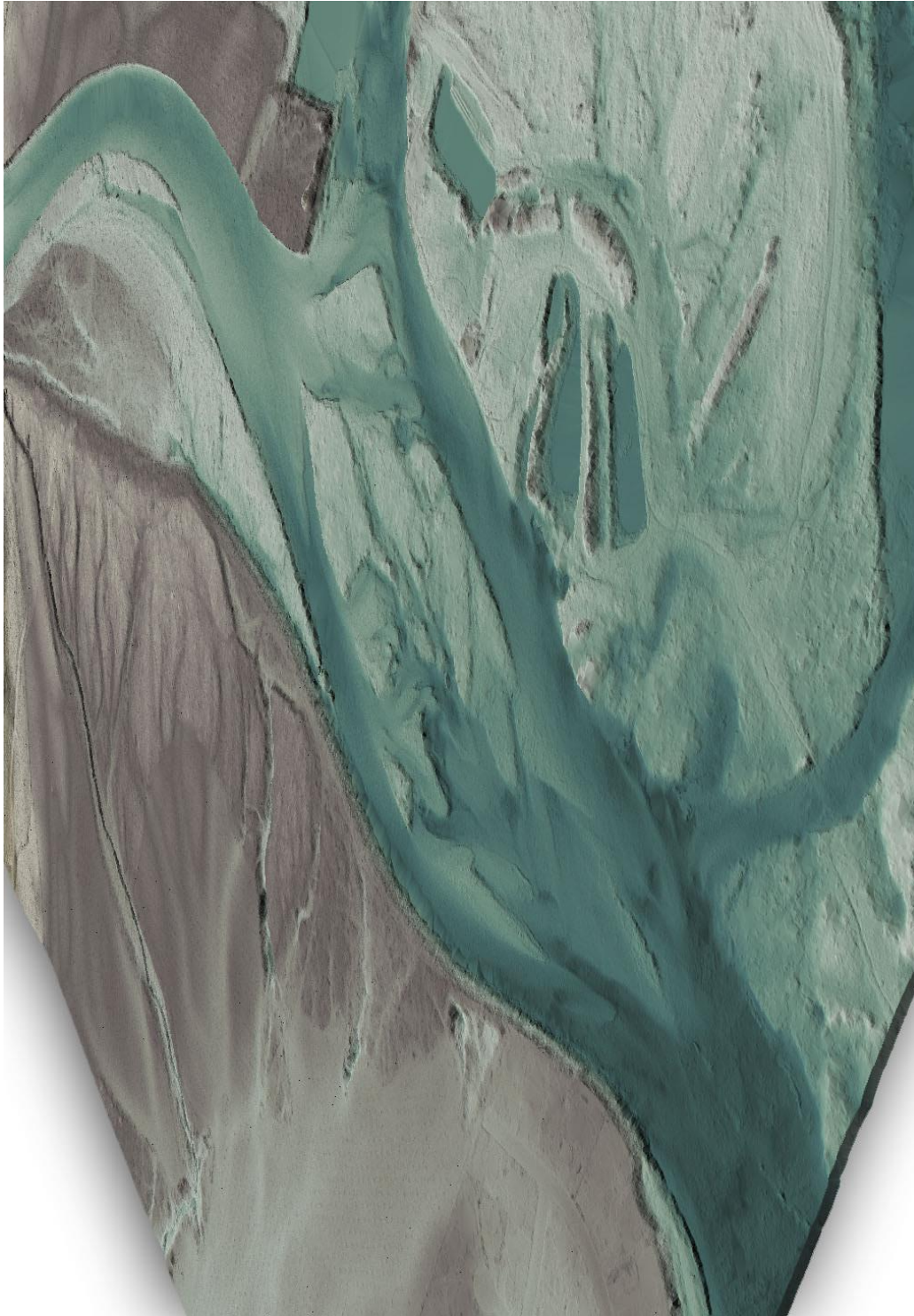


Figure 19: Confluence of the Willamette and Coast Fork Willamette Rivers looking east. The scene is created from the gridded ground and bathymetry classified LiDAR returns colored by height.

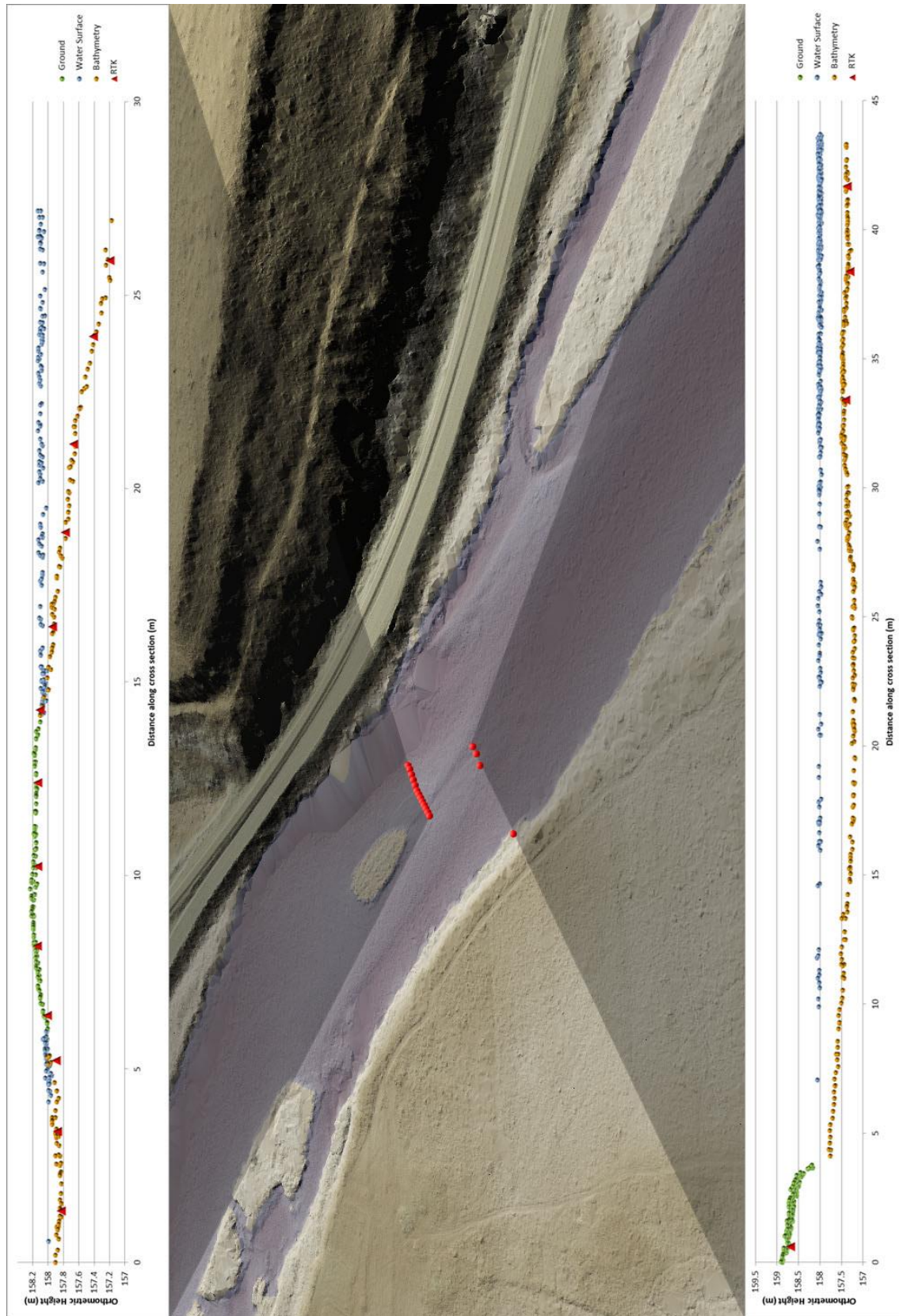


Figure 20: View of RTK survey area along the Willamette River. The cross section highlights the congruity between the LiDAR returns and RTK survey.

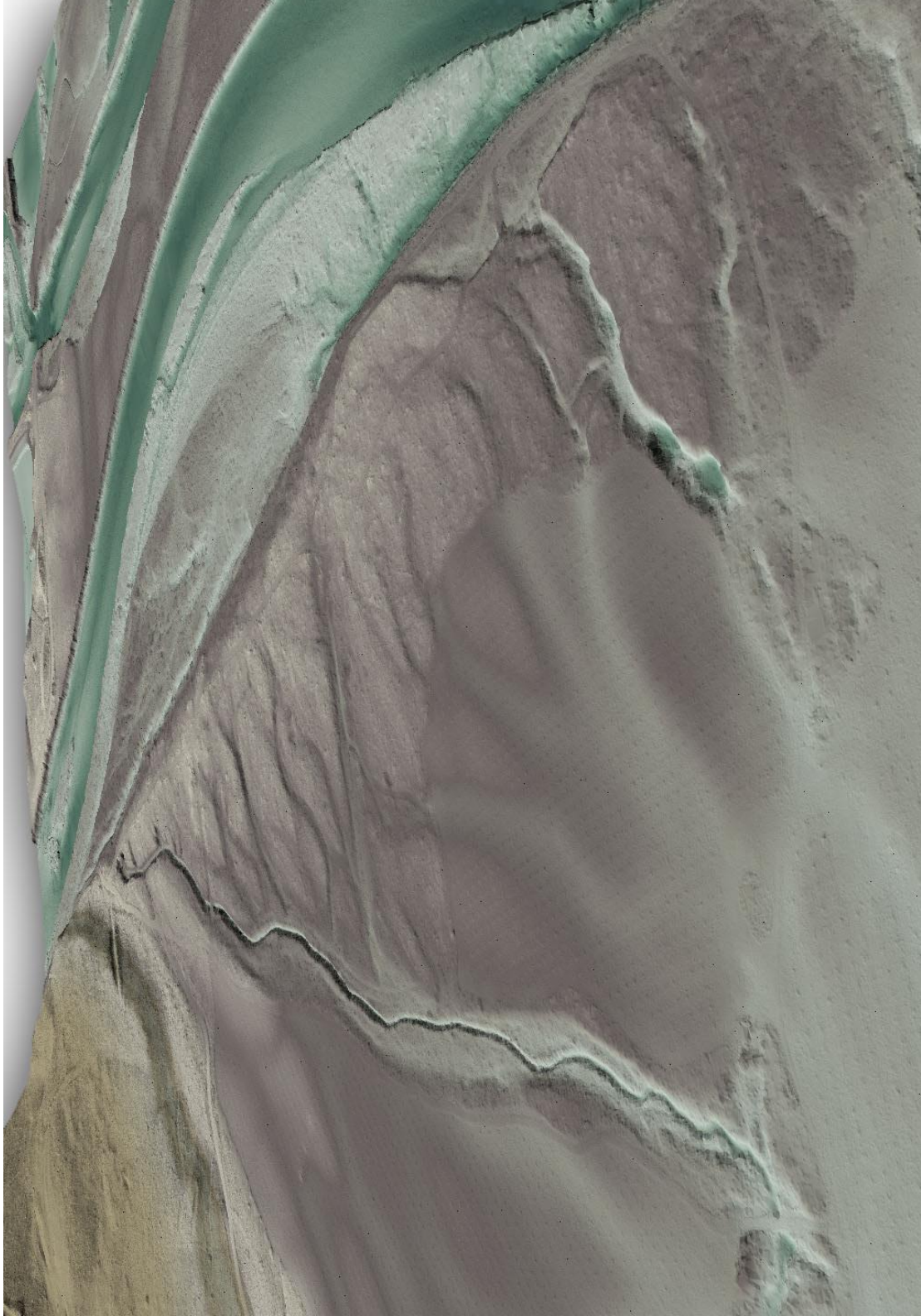


Figure 21: Confluence of the Willamette and Coast Fork Willamette Rivers. The scene is created from the gridded ground and bathymetry classified LiDAR returns colored by height.

1-sigma (σ) Absolute Deviation: Value for which the data are within one standard deviation (approximately 68th percentile) of a normally distributed data set.

1.96 * RMSE Absolute Deviation: Value for which the data are within two standard deviations (approximately 95th percentile) of a normally distributed data set, based on the FGDC standards for Fundamental Vertical Accuracy (FVA) reporting.

Accuracy: The statistical comparison between known (surveyed) points and laser points. Typically measured as the standard deviation (sigma σ) and root mean square error (RMSE).

Absolute Accuracy: The vertical accuracy of LiDAR data is described as the mean and standard deviation (sigma σ) of divergence of LiDAR point coordinates from ground survey point coordinates. To provide a sense of the model predictive power of the dataset, the root mean square error (RMSE) for vertical accuracy is also provided. These statistics assume the error distributions for x, y and z are normally distributed, and thus we also consider the skew and kurtosis of distributions when evaluating error statistics.

Relative Accuracy: Relative accuracy refers to the internal consistency of the data set; i.e., the ability to place a laser point in the same location over multiple flight lines, GPS conditions and aircraft attitudes. Affected by system attitude offsets, scale and GPS/IMU drift, internal consistency is measured as the divergence between points from different flight lines within an overlapping area. Divergence is most apparent when flight lines are opposing. When the LiDAR system is well calibrated, the line-to-line divergence is low (<10 cm).

Root Mean Square Error (RMSE): A statistic used to approximate the difference between real-world points and the LiDAR points. It is calculated by squaring all the values, then taking the average of the squares and taking the square root of the average.

Data Density: A common measure of LiDAR resolution, measured as points per square meter.

Digital Elevation Model (DEM): File or database made from surveyed points, containing elevation points over a contiguous area. Digital terrain models (DTM) and digital surface models (DSM) are types of DEMs. DTMs consist solely of the bare earth surface (ground points), while DSMs include information about all surfaces, including vegetation and man-made structures.

Intensity Values: The peak power ratio of the laser return to the emitted laser, calculated as a function of surface reflectivity.

Nadir: A single point or locus of points on the surface of the earth directly below a sensor as it progresses along its flight line.

Overlap: The area shared between flight lines, typically measured in percent. 100% overlap is essential to ensure complete coverage and reduce laser shadows.

Pulse Rate (PR): The rate at which laser pulses are emitted from the sensor; typically measured in thousands of pulses per second (kHz).

Pulse Returns: For every laser pulse emitted, the number of wave forms (i.e., echos) reflected back to the sensor. Portions of the wave form that return first are the highest element in multi-tiered surfaces such as vegetation. Portions of the wave form that return last are the lowest element in multi-tiered surfaces.

Real-Time Kinematic (RTK) Survey: A type of surveying conducted with a GPS base station deployed over a known monument with a radio connection to a GPS rover. Both the base station and rover receive differential GPS data and the baseline correction is solved between the two. This type of ground survey is accurate to 1.5 cm or less.

Post-Processed Kinematic (PPK) Survey: GPS surveying is conducted with a GPS rover collecting concurrently with a GPS base station set up over a known monument. Differential corrections and precisions for the GNSS baselines are computed and applied after the fact during processing. This type of ground survey is accurate to 1.5 cm or less.

Scan Angle: The angle from nadir to the edge of the scan, measured in degrees. Laser point accuracy typically decreases as scan angles increase.

Native LiDAR Density: The number of pulses emitted by the LiDAR system, commonly expressed as pulses per square meter.

APPENDIX A - ACCURACY CONTROLS

Relative Accuracy Calibration Methodology:

Manual System Calibration: Calibration procedures for each mission require solving geometric relationships that relate measured swath-to-swath deviations to misalignments of system attitude parameters. Corrected scale, pitch, roll and heading offsets were calculated and applied to resolve misalignments. The raw divergence between lines was computed after the manual calibration was completed and reported for each survey area.

Automated Attitude Calibration: All data were tested and calibrated using TerraMatch automated sampling routines. Ground points were classified for each individual flight line and used for line-to-line testing. System misalignment offsets (pitch, roll and heading) and scale were solved for each individual mission and applied to respective mission datasets. The data from each mission were then blended when imported together to form the entire area of interest.

Automated Z Calibration: Ground points per line were used to calculate the vertical divergence between lines caused by vertical GPS drift. Automated Z calibration was the final step employed for relative accuracy calibration.

LiDAR accuracy error sources and solutions:

Type of Error	Source	Post Processing Solution
GPS (Static/Kinematic)	Long Base Lines	None
	Poor Satellite Constellation	None
	Poor Antenna Visibility	Reduce Visibility Mask
Relative Accuracy	Poor System Calibration	Recalibrate IMU and sensor offsets/settings
	Inaccurate System	None
Laser Noise	Poor Laser Timing	None
	Poor Laser Reception	None
	Poor Laser Power	None
	Irregular Laser Shape	None

Operational measures taken to improve relative accuracy:

Low Flight Altitude: Terrain following was employed to maintain a constant above ground level (AGL). Laser horizontal errors are a function of flight altitude above ground (about 1/3000th AGL flight altitude).

Focus Laser Power at narrow beam footprint: A laser return must be received by the system above a power threshold to accurately record a measurement. The strength of the laser return (i.e., intensity) is a function of laser emission power, laser footprint, flight altitude and the reflectivity of the target. While surface reflectivity cannot be controlled, laser power can be increased and low flight altitudes can be maintained.

Reduced Scan Angle: Edge-of-scan data can become inaccurate. The scan angle was reduced to a maximum of $\pm 21^\circ$ from nadir, creating a narrow swath width and greatly reducing laser shadows from trees and buildings.

Quality GPS: Flights took place during optimal GPS conditions (e.g., 6 or more satellites and PDOP [Position Dilution of Precision] less than 3.0). Before each flight, the PDOP was determined for the survey day. During all flight times, a dual frequency DGPS base station recording at 1 second epochs was utilized and a maximum baseline length between the aircraft and the control points was less than 13 nm at all times.

Ground Survey: Ground survey point accuracy (<1.5 cm RMSE) occurs during optimal PDOP ranges and targets a minimal baseline distance of 4 miles between GPS rover and base. Robust statistics are, in part, a function of sample size (n) and distribution. Ground survey points are distributed to the extent possible throughout multiple flight lines and across the survey area.

50% Side-Lap (100% Overlap): Overlapping areas are optimized for relative accuracy testing. Laser shadowing is minimized to help increase target acquisition from multiple scan angles. Ideally, with a 50% side-lap, the nadir portion of one flight line coincides with the swath edge portion of overlapping flight lines. A minimum of 50% side-lap with terrain-followed acquisition prevents data gaps.

Opposing Flight Lines: All overlapping flight lines have opposing directions. Pitch, roll and heading errors are amplified by a factor of two relative to the adjacent flight line(s), making misalignments easier to detect and resolve.